Role of Higher-order Inertia in Modulating Elastic Wave Dispersion in Materials with Granular Microstructure

Nima Nejadsadeghi[1] and Anil Misra[2*]

[1]Mechanical Engineering Department,
University of Kansas, 1530 W 15th Street, Learned Hall, Lawrence, KS 66047-7609
[2]Civil, Environmental and Architectural Engineering Department,
University of Kansas, 1530 W 15th Street, Learned Hall, Lawrence, KS 66045-7609.
*corresponding author: Ph: (785) 864-1750, Fax: (785) 864-5631, Email: amisra@ku.edu

For possible publication in:

International Journal of Mechanical Sciences

Abstract

(Meta-) materials with granular microstructures exhibit nonlinear dispersive wave propagation, which is typically attributed to the presence of a microstructure. However, this behavior can arise from two additional sources in a linear non-dissipative system – the grain-scale or micromechanical characteristics and the grain-scale or micro-inertial characteristics. The microstructure, the grain-scale mechanical and the grain-scale inertial properties in combination may be designated as micro-mechano-morphology. From a continuum modeling viewpoint, the observed dispersion behavior that accounts for micro-mechano-morphology of materials with granular microstructures can be described using a granular micromechanics based micromorphic model (Nejadsadeghi and Misra 2019b, Misra and Poorsolhjouy 2016). Following the approach outlined in these works, we elaborate on the effect of micro-scale inertia upon the wave propagation behavior. The work is motivated by the observation of negative group velocity of optical waves seen in simulations using discrete models of granular media. We show that higher-order inertia is necessary for describing this phenomena using continuum models. We further show that this phenomena can be modulated by micro-scale mass density distributions, thus affecting the widths of potential frequency band-gaps, including the negative group velocity of the acoustic branch.

Keywords: granular microstructure; granular micromechanics; higher-order inertia; dispersion relation; frequency band gaps; granular metamaterials.

1. Introduction

1.1 Micro-mechano-morphological effects

Materials with granular microstructure are characterized as materials composed of many individual grains mediated by interfaces. Due to their prevalence in diverse areas of engineering and science, it is necessary to promote the understanding on how such materials behave when excited externally. In addition to the materials with granular microstructure found in nature, recently emerged *granular metamaterials* also share many features with granular solids and are worth studying, especially for vibration mitigation applications [1,2]. The collective behavior of granular structures (granular solids and granular metamaterials) is mainly connected to their micro-mechano-morphology. In other words, grain-pair interactions, composition and morphological aspects of granular structures in micro-scale dictate their macro-scale mechanical behavior. While for problems consisting of hundreds to thousands of grains a discrete model may be utilized [3–5], as the size of the structure grows (e.g. for granular structures comprising millions of grains) continuum models remain the most efficient. Continuum description of a material with granular microstructure expresses the macroscopic behavior of the material in an averaged sense based on the microstructural properties of the structure in a less computationally expensive manner. Indeed, continuum models do not predict the trajectory of each grain inside the granular structure. However, given the incomplete information about the granular structure in terms of the grain-pair interaction properties and the accurate positions and geometries for all the grains in contact, an approximate description based on insufficient data is adequate.

Classical continuum mechanics declares a material point with its size approaching zero. Such a description is enough to describe and characterize the local effects (immediate neighborhood). However, the complexity of the granular medium in both mechanical and morphological aspects necessitates a refined description of the behavior of granular materials that takes into account the non-local effect of grain-interactions [6] and grain rotations [7], to predict phenomena such as dispersion in propagating elastic waves [8–12]. Dispersion in waves propagating through granular structures is pertinent to the existence of an inherent characteristic length comparable to the wavelength of excitation at high frequencies [9,13]. The characteristic length is often attributed to granular materials microstructural aspects (see for example [14]), however, it should

also account for the micro- or grain-scale mechanical characteristics and the micro- or the grain-scale inertial characteristics. The microstructure, the grain-scale mechanical and the grain-scale inertial properties in combination can be designated as micro-mechano-morphology. It is, therefore, imperative to include the information about the granular material's micro-mechano-morphology in formulating the continuum wave equations. Granular micromechanics approach (GMA) results in a non-classical continuum mechanics model for describing the mechanical behavior of granular structures considering the micro-mechano-morphological effects using refined kinematics [6,15]. As a generalization of the classical continuum mechanics viewpoint, a material point in GMA is considered a collection of grains interacting with each other via different inter-granular mechanisms. The GMA treats the problem in a statistical sense by considering the mean behavior of grain pairs.

1.2 Motivation

In its most general forms, the GMA leads to micromorphic models of degree n [6], and treats grain-spins using as independent kinematic quantities [7]. In its simplest form, the GMA devolves to the classical Cauchy-form of continuum models. In our earlier publications, we have studied the elastic wave propagation in a material with granular microstructure utilizing GMA based micromorphic theory of degree 1 described in [6,15]. The results from our previous work [9] have shown interesting information about wave propagation in granular media. These include wave dispersion as well as the occurrence of a slow longitudinal wave that follows the primary longitudinal wave as seen in the discrete simulations reported by [5]. It is noteworthy, however, that in nonlinear-dissipative systems (as in [5]), wave dispersion may be affected by multiple dissipation mechanisms (including viscous, frictional dissipation at the grain scales), and therefore, can depend upon the loading history in addition to the micro-mechano-morphology. The relative influences of these factors need careful investigations. The GMA based continuum model provides a systematic way to explore the influences of the many confounding factors, such as grain-pair elastic and dissipative interactions and grain inertia, which influence the macro-scale behavior of granular systems [6,7,16]. For example, longitudinal and transverse elastic wave propagation in 1D granular materials studied using GMA based model revealed the existence of multiple wave branches in both forward and backward waves, dispersion in wave

propagation, where waves with different frequencies propagate with different velocities, and the possibility of the existence of frequency band gaps [9]. This model, enhanced to account for the effect of the external electric field, showed the possibility of modulating and tuning wave dispersion in granular materials composed of dielectric grains [8]. Thus, the GMA based continuum model can serve as a basis for designing experiments as well as discrete simulations. To this end, we note that our previous model failed to capture completely certain aspects of phononic negative group velocity (NGV) that are predicted by discrete models and recent works on wave propagation characteristics in granular media, e.g., [17].

We remark that phononic waves with NGV are known for 1D composite materials described by Rytov model of layered system using wave equations of classical continuum mechanics and specification of the layer properties [18–20]. The phenomenon of NGV has also been observed in other systems. For example, the appearance of NGV has been recognized in layered materials in electromagnetics [21] and in metamaterials with negative permittivity and negative permeability [22]. In soft composites, NGV in transverse or shear waves is believed to cause elastic instabilities in fibrous composites [23]. In elastic composites with periodic microstructure, NGV was accomplished by utilizing the idea of local resonances to produce low-frequency negative passband [24], or by embedding stiff inclusions in soft matrix [25]. NGV was also observed in 2D metamaterials modeled as mass spring systems with nonlocal effect [26] and in 1D lattice chain incorporating nonlocal effects [27]. Moreover, in solids with multi-scale microstructure, NGV is predicted for particular material parameters [28]. The present paper focuses upon granular materials that are homogeneous at the scale of investigation but are microscopically inhomogeneous. The aim of the present work is to develop non-classical wave equations that addresses different aspects of wave dispersion in macroscopically homogeneous granular systems.

To illustrate the issue of negative group velocity in granular media, we consider a discrete bead-spring model of 20 grains as shown in Fig. 1a. This set of grains are taken to comprise the representative volume element (RVE) of an infinitely extending 1D granular material. The grain-pair interactions are modeled as linear elastic springs (denoted as $k_i, i = 1, 2, ..., n$) whose stiffnesses have no asymmetry under tension or compression (such that the grains maintain enduring interactions during the wave propagation). Further, the spring stiffnesses are randomly

distributed in a prescribed range and the grains are treated as rigid masses (denoted as $m_i, i = 1,2,...,n$) of radius of 0.5 mm with varying grain mass densities. The distributions of grain-pair stiffnesses and grain mass densities used in our discrete simulations are shown in Fig. 1b and Fig. 1c. The dispersion curve of the considered structure can be now calculated from the equations of motion for grains in the RVE, assuming a harmonic form of solution for their displacement, and applying periodic boundary conditions. The computed dispersion relation for this model in the irreducible Brillouin zone is illustrated in Fig. 2a. The dispersion curve shown here has as many wave branches as the degrees of freedom in the RVE. Here we focus upon the dispersion curves for the first two wave branches, one optical and the other acoustic, replotted in Fig. 2b, which are at the lowest frequency range for comparison with the lowest frequency modes that have been predicted by the GMA based micromorphic model of degree 1 [9]. The acoustic branch in both models (discrete model and the model in [9]) shows similar characteristics. However, the optical branch predicted by the discrete simulation shows negative group velocity, which is in contrast to the previous format of GMA [9] which predicts positive and increasing group velocity.

This apparent discrepancy in predictions by the GMA based continuum model can be resolved by recognizing the existence of higher order inertia terms that appear in GMA based micromorphic theory of degree 1 as shown in our recent work on extended granular micromechanics approach [6]. We note that NGV is also predicted using classical micromorphic continuum models, by considering the cross-linking terms between macro- and micro-scale kinematic variables [29,30]. In contrast, the models that do not consider these cross-linking terms predict positive group velocity in the optical branch [9,31,32]. In the present paper, we show that models that do not consider the cross-linking of macro- and micro-scale kinematic variables terms but include higher order inertia terms also predict NGV. Notably, the higher-order inertia term is, typically, absent in the classical micromorphic theories of degree 1, although such inertial terms are often included in 2nd gradient elasticity (see for example [33–36]). The higher order inertia terms arise from the variations in the micro-inertial properties as a combined effect of grain-sizes, compositions and the grain scale morphology (granular arrangement). Vibration and wave propagation characteristics of granular systems have been shown to be affected by specific granular arrangements and varying grain sizes in the recent works of [37–39]. In particular, mass ratio of the grains within a diatomic granular structure has been shown to affect

the width and location of the frequency band gap, which reveals the micro-inertial effects on the band structure [17]. However, to the knowledge of the authors, no study has yet been done to generalize the micro-inertial influence on the propagating waves in a granular structure. To this end, we introduce an extended form of kinetic energy that includes the rates of micro-scale kinematic measures and its conjugate higher order micro-inertia. Our aim in the present paper is to highlight the role of higher order micro-inertia terms in the dispersive behavior of granular materials through the example of wave propagation in an infinite 1D continuum with granular microstructure. In particular, we illustrate how the grain mass density distribution can lead to modulation of the dynamic behavior of materials with granular microstructure. A 1D system proves to be expedient in describing the physics involved in the problem while reducing the complexity of the system under study, compared to a general 3D case.

The organization of the paper is as follows. An overview of the granular micromechanics approach is provided in section 2, where the kinematics of GMA based micromorphic theory of degree 1 and the variational approach to obtain the balance equations are described. Section 3 is devoted to study the longitudinal elastic wave propagation in a 1D material with granular microstructure taking into account the effect of higher order inertia terms. Finally, section 4 presents the summary of the work and the concluding remarks.

2. GMA based micromorphic theory of degree 1

2.1. Kinematic variables

In this section, we briefly introduce the continuum framework for GMA. The reader is referred to the references [6,15] for an extensive description of the approach. In GMA, a granular structure is considered as a continuum with the volume V bounded by the surface S where the material point P can be identified using a macro-scale Euclidean coordinate system x_i (see Fig. 3). The material point P is assumed to have the macro-scale mass density ρ, volume $dV = V'$, and differential mass $dm = \rho dV = \rho V'$. Denoting by $\mathbf{X}$ and $\mathbf{x} = \boldsymbol{\chi}(\mathbf{X}, t)$ the position vectors of the point P at initial and current configurations (at time t), respectively, the macro-scale displacement vector $\mathbf{u}$ ascribed to the point P is defined as $\mathbf{u} = \mathbf{x} - \mathbf{X}$. The material point P,

microscopically, is an assemblage of grains and can be referred to as a statistical/representative volume element (RVE) with volume $dV = V'$. The positions of grains inside the RVE can be distinguished utilizing a micro-scale coordinate system x_i' attached to the center of mass (COM) of the material point P, parallel to the macro-scale coordinate system x_i, and moving with the macro-scale displacement **u**. Denoting by $\mathbf{X}'$ and $\mathbf{x}' = \boldsymbol{\chi}'(\mathbf{X}, \mathbf{X}', t)$ the position vectors of the grain p centroid at initial and current configurations, respectively, the micro-scale displacement vector $\mathbf{u}'$ ascribed to the grain p is defined as $\mathbf{u}' = \mathbf{x}' - \mathbf{X}'$.

In the current format of GMA, we consider, in both micro- and macro-scales, infinitesimal deformation in granular media. We also assume that macro-scale and micro-scale displacements are both continuous and differentiable functions of x_i and x_i' up to the desired order. Therefore, we have the following form for the macro- and micro-scale displacements

$$u_i = u_i\left(x_j, t\right), \quad u_i' = u_i'\left(x_j, x_j', t\right). \tag{1}$$

For a micromorphic theory of degree 1, the micro-scale displacement u_i' can be written using a polynomial expansion and keeping up to the second order terms with respect to $\mathbf{x}'$ about the COM of the RVE as [6]

$$u_i' = \psi_{ij} x_j' + \psi_{ijk} x_j' x_k'. \tag{2}$$

In Eq. (2), ψ_{ij} and ψ_{ijk} are, respectively, second and third rank micro-deformation tensors only functions of $\mathbf{x}$ and *t*. In Eq. (2) and henceforward, summation convention over repeated indices is implied unless noted otherwise. Without loss of generality, we further assume that the micro-deformation tensor ψ_{ijk} is symmetric with respect to indices *j* and *k* [6,40]. With regards to Eq. (2), the total displacement vector for the grains inside the RVE can be written as

$$\phi_i = u_i + u_i' = \bar{\phi}_i + \psi_{ij} x_j' + \psi_{ijk} x_j' x_k'. \tag{3}$$

where $\bar{\phi}_i = u_i$ is adopted to harmonize the variable names with previous publications [6,8–10,15]. We introduce the following relative deformation tensors [6,30,40]

$$\gamma_{ij} = \bar{\phi}_{i,j} - \psi_{ij}, \quad \gamma_{ijk} = \psi_{ij,k} - \psi_{ijk}, \tag{4}$$

where, henceforth, comma in the subscript denotes differentiation with respect to the spatial coordinates. In Eq. (4), the differentiation is taken with respect to the macro-scale coordinate system basis vectors. For a micromorphic theory of degree 1, and as a constitutive choice, we assume that the relative deformation tensor γ_{ijk} is zero. Such an assumption reads $\psi_{ijk} = \psi_{ij,k}$. As noted in [6], this assumption changes the independent nature of ψ_{ijk} to a dependent one. We further note that under additional assumptions of vanishing relative deformation tensor γ_{ij}, the theory will devolve to a 2nd gradient theory, which is known to have wide applications [41–43] and has been deduced through homogenization of certain lattice structures (see for example [44–46]).

For the neighboring grains n and p, utilizing Eq. (3) and Eq. (4), the relative displacement between grains can be decomposed as

$$\delta_i^{\mathrm{np}} = \phi_i^{\mathrm{p}} - \phi_i^{\mathrm{n}} = \delta_i^{\mathrm{M}} - \delta_i^{\mathrm{m}} + \delta_i^{\mathrm{g}}, \tag{5}$$

where the following micro-scale kinematic measures are recognized

$$\delta_i^{\mathrm{M}} = \bar{\phi}_{i,j} J_j^{\mathrm{np}}, \quad \delta_i^{\mathrm{m}} = \gamma_{ij} J_j^{\mathrm{np}}, \quad \delta_i^{g} = \psi_{ij,k} J_{jk}^{\mathrm{np}}. \tag{6}$$

In Eq. (5) and Eq. (6), we have defined the geometry moment measures $J_j^{\mathrm{np}} = l_j^{\mathrm{p}} - l_j^{\mathrm{n}}$ and $J_{jk}^{\mathrm{np}} = l_j^{\mathrm{p}} l_k^{\mathrm{p}} - l_j^{\mathrm{n}} l_k^{\mathrm{n}}$, where l_j^{q} represents the j^{th} component of the vector joining the COM of the RVE to the grain q centroid. Moreover, δ^{M} indicates the part of the relative displacement due to the macro-scale displacement gradient, δ^{m} denotes the portion of the relative displacement due to the fluctuation between the macro-scale gradient $\bar{\phi}_{,x}$ and the micro-scale kinematic measure ψ, and δ^{g} represents the part of the relative displacement due to the second gradient.

The macro-scale rotation, $\bar{\kappa}_i$, in the macro-scale coordinate system is defined as

$$\bar{\kappa}_i = \frac{1}{2} e_{lki} u_{k,l} = \frac{1}{2} e_{lki} \bar{\phi}_{k,l}, \tag{7}$$

where the differentiation is with respect to the macro-scale coordinate system x_i and e_{lki} is the permutation symbol. Similarly, the micro-scale rotation, $\hat{\imath}_i$, in the micro-scale coordinate system is defined as

$$\hat{\imath}_i \quad 2^{-\iota\kappa\iota\cdots}{}_{k,l}' = \frac{1}{2} e_{lki} \phi_{k,l}, \tag{8}$$

where the differentiation is with respect to the micro-scale coordinate system x_i'. The relative rotation of two neighboring grains n and p inside the material point P only takes into account the effect of the micro-scale rotation, $\hat{\imath}_i$. We note here that the grain spin effect is not considered in the current formulation of GMA. Utilizing Eq. (8), the relative rotation between two neighboring grains n and p, θ_i^u, can be written as

$$\theta_i^u = e_{lki} \psi_{kl,j} J_j^{\mathrm{np}}. \tag{9}$$

The micro-scale kinematic measures introduced in Eq. (6) and Eq. (9) are considered deformation mechanisms in which the deformation energy is stored.

2.2. Constitutive equations

We assume the macro-scale deformation energy density to be a function of the macro-scale kinematic measures, i.e., of the form $W = W(\bar{\phi}_{(i,j)}, \gamma_{ij}, \psi_{ij,k})$, where $\bar{\phi}_{(i,j)}$ is the symmetric part of the macro-scale displacement gradient. Considering the assumed form of the macro-scale deformation energy density with its mentioned components ensures an objective expression for the energy density that is invariant to rigid rotation of the coordinate system. The macro-scale stress measures of Cauchy stress, relative stress, and double stress are defined as conjugates to the continuum kinematic measures, respectively as

$$\tau_{ij} = \frac{\partial W}{\partial \bar{\phi}_{(i,j)}}, \quad \sigma_{ij} = \frac{\partial W}{\partial \gamma_{ij}}, \quad \mu_{ijk} = \frac{\partial W}{\partial \psi_{ij,k}}. \tag{10}$$

The macro-scale deformation energy density can be identified in terms of the micro-scale deformation energy density as

$$W = \frac{1}{V'}\sum_{\alpha} W^{\alpha}\left(\delta_i^{\alpha \mathrm{M}}, \delta_i^{\alpha \mathrm{m}}, \delta_i^{\alpha \mathrm{g}}, \theta_i^{\alpha \mathrm{u}}\right), \tag{11}$$

where W^{α} represents the micro-scale deformation energy for the α^{th} interacting pair of grains. Intergranular forces and moments can be defined as conjugates to the micro-scale kinematic measures as

$$\frac{\partial W}{\partial \delta_i^{\alpha\zeta}} = f_i^{\alpha\zeta}; \quad \zeta = \mathrm{M,m,g}, \quad \frac{\partial W}{\partial \theta_i^{\alpha \mathrm{u}}} = m_i^{\alpha \mathrm{u}}. \tag{12}$$

Substituting Eq. (11) into Eq. (10), and using Eq. (6), Eq. (9), and Eq. (12), it follows that the macro-scale stress measures can be expressed in terms of the intergranular forces and moments and the geometry moment measures [15]. For a non-dissipative linear system a quadratic form of micro-scale deformation energy density W^{α} can be considered. To this end, the micro-scale kinematic measures in Eq. (6) and Eq. (9) can be decomposed into their normal (n) and two other tangential (s and t) components, with the normal being along the direction of the line connecting the centroids of the two grains. As an example, the micro-scale deformation energy density used in this paper can be expressed in the quadratic form $W^{\alpha} = \frac{1}{2}\sum_{\zeta}\sum_{i} K_i^{\alpha\zeta}\left(\delta_i^{\alpha\zeta}\right)^2 + \frac{1}{2}\sum_{i} G_i^{\alpha u}\left(\theta_i^{\alpha u}\right)^2$ with $i = n,s,t$, and $\zeta = \mathrm{M,m,g}$, and where different K and G parameters represent grain-pair stiffness parameters for the macro-scale, M, micro-scale, m, and second gradient, g, mechanisms involved in the deformation [15]. We note that the assumed form for the micro-scale deformation energy density W^{α} does not consider the terms that cross-link different micro-scale kinematic measures in the current analysis. The assumed form of micro-scale deformation energy density, W^{α}, leads to the macro-scale constitutive relationships presented below [15,47]

$$\tau_{ij} = C_{ijkl}^{\mathrm{M}}\varepsilon_{kl}, \quad \sigma_{ij} = C_{ijkl}^{\mathrm{m}}\gamma_{kl}, \quad \mu_{ijk} = \left(A_{ijklmn}^{\mathrm{g}} + A_{ijklmn}^{\mathrm{u}}\right)\psi_{lm,n}. \tag{13}$$

In Eq. (13), C_{ijkl}^{M} and C_{ijkl}^{m} are fourth rank stiffness tensors, and A_{ijklmn}^{g} and A_{ijklmn}^{u} are sixth rank stiffness tensors, defined as functions of the grain-pair interaction stiffnesses K and G and geometry moment measures for all the grain pairs within the RVE. In Eq. (13), the superscript M denotes macro-stiffness, m denotes the micro-stiffness, g denotes the second gradient stiffness, and u represents the rotational stiffness.

2.3. Governing equations of motion

In this paper, we obtain the equations of motion based on the principle of stationary action. Hamilton's principle states that the action functional is minimum, and is expressed as

$$\delta\int_{t_0}^{t_1}\left(\tilde{T} \quad \tilde{V} \quad \tilde{V}\right) \quad , \tag{14}$$

where the terms $\tilde{T}$, $\tilde{V}$, and $\tilde{V}$ are defined in what follows. $\tilde{T}$ is the total kinetic energy, where T is the kinetic energy density, utilizing König's theorem [48] defined as [6]

$$T = \frac{1}{V'}\int_{V'}\frac{1}{2}\rho'\dot{\zeta} \qquad \frac{1}{2}\rho\dot{\zeta} \qquad \frac{1}{2}\rho\dot{y} \tag{15}$$

In Eq. (14), ρ' is the micro-scale mass density per unit macro-volume, which can be non-uniform within the RVE (a function of the micro-scale coordinate system x_i'), and each over-dot henceforward represents differentiation with respect to the temporal coordinate. Moreover, the following inertia measures have been defined [6]

$$\rho = \frac{1}{V'}\int_{V'}\rho' dV', \quad \rho_{jm} = \frac{1}{V'}\int_{V'}\rho' x_j' x_m' dV', \quad \rho_{jmn} = \frac{1}{V'}\int_{V'}\rho' x_j' x_m' x_n' dV', \quad \rho_{jkmn} = \frac{1}{V'}\int_{V'}\rho' x_j' x_k' x_m' x_n' dV' \tag{16}$$

where, clearly, the macro-scale mass density ρ and other measures of inertia depend on the micro-scale mass density ρ' and its distribution within the RVE. In what follows, we consider that the material is homogenous at the macro-scale, that is the macro-scale mass density ρ is independent of the macro-scale coordinate system, x_i. The kinetic energy density defined in Eq. (15) is an extension of the ones introduced in earlier publications for GMA based micromorphic theory of degree 1, e.g. in [8–10,15]. The additional terms in the description of the kinetic energy affect the prediction of the dynamic behavior of granular media by introducing, or re-allocating, energies in the existing degrees of freedom of the problem. Moreover, the additional terms are accompanied by higher order inertia measures that were otherwise absent in [8–10,15]. Clearly, the micro-scale mass density distribution in the RVE can alter the higher order inertia measures,

while potentially keeping the macro-scale mass density ρ constant. This allows us to imagine two morphologically different systems with identical constituents and equal macro-scale mass density showing different wave propagation characteristics or two morphologically identical systems with different constituents and equal macro-scale mass density showing different wave propagation characteristics. This reveals (micro-) morphological and compositional effects on vibration characteristics of granular media. Now if the grain-pair interactions between all constituent grains are kept constant, the dynamic properties of the granular medium changes solely because of the change in inertia measures. This aspect is elaborated in the following sections.

In Eq. (14), $\tilde{V}$ [illegible] is the total macro-scale deformation energy, and $\tilde{V}$ is the total external energy where its form is inspired by the expression for the total macro-scale deformation energy $\tilde{V}$, with components described below. Thus from Eq. (14) we get [6]

$$\begin{aligned}&\int_{t_0}^{t_1}\int_V \Big[\left(\tau_{ij}+\sigma_{ij}\right)_{,j}+f_i-\rho\ddot{\ }\Big]\ddot{\ }\ dt+\int_{t_0}^{t_1}\int_V \Big[\sigma_{ij}+\mu_{ijk,k}+\Phi_{ij}-\rho_{jk}\ddot{\ }\ \ddot{\ }\ \Big]dVdt\\&+\int_{t_0}^{t_1}\int_S \Big[t_i-\left(\tau_{ij}+\sigma_{ij}\right)n_j\Big]\delta\bar{\phi}_i dSdt+\int_{t_0}^{t_1}\int_S \Big[T_{ij}-\left(\rho_{jkl}\ddot{\ }\ \ddot{\ }\ \right)n_k\Big]\delta\psi_{ij}dSdt=0\end{aligned} \tag{17}$$

In Eq. (17), f_i is the non-contact body force per unit volume, t_i is the contact traction defined as a surface force per unit area, Φ_{ij} is the non-contact body double force per unit volume, and T_{ij} is the contact double traction defined as double force per unit area. Moreover, n_j represents the j^{th} component of the normal to the surface *S*. In what follows, we assume zero non-contact body forces and double forces.

Equations of motion and natural boundary conditions are obtained, utilizing the fundamental lemma of calculus of variations and the constitutive relations in Eq. (13), as

$$\left(C^M_{ijkl}+C^m_{ijkl}\right)\bar{\phi}_{k,lj}-C^m_{ijkl}\psi_{kl,j}=\rho\ddot{\ }, \tag{18a}$$

$$\left(A^g_{ijklmn}+A^u_{ijklmn}\right)\psi_{lm,nk}+C^m_{ijkl}\bar{\phi}_{k,l}-C^m_{ijkl}\psi_{kl}=\rho_{jk}\ddot{\ }\ \ddot{\ }\ , \tag{18b}$$

$$\left(\tau_{ij}+\sigma_{ij}\right)n_j=t_i \tag{19a}$$

$$\left(\rho_{jkl}\ddot{u}_{\quad}-\ddot{u}_{\quad}\right)n_k = T_{ij} \tag{19b}$$

It is noteworthy that the term $\rho_{jklm}\ddot{u}_{\quad}$ in Eq. (18b) is typically not considered in micromorphic models of degree 1, such as the previous models found in [8–10]. We further note that the 3rd rank inertial tensor appears in the boundary conditions and not in the governing equations. Note that in the 2nd gradient theory presented in [49], the 3rd rank inertial tensor appears in the governing equation, while there is no discussion of the boundary conditions.

3. Longitudinal elastic wave propagation in a 1D continuum with granular microstructure

We here focus on the longitudinal wave propagation in an infinite 1D continuum in macro- and micro-scales along the x_1 axis. A representation of the general problem is shown in Fig. 4, where different grain colors represent different micro-scale mass density ρ' and elastic properties. For brevity, we drop the subscript 1 from the axis x_1 and denote it by *x*. Similarly, we represent $\bar{\phi}_1$ and ψ_{11} by $\bar{\phi}$ and ψ, and C^M_{1111}, C^m_{1111}, and A^g_{111111} by C^M, C^m, and A^g, respectively. Note that in the 1D case under study, $A^u_{111111}=0$ [15]. The equations of motion, Eq. (18), for the current 1D case reduce to the following equations

$$\left(C^M+C^m\right)\bar{\phi}_{,xx}-C^m\psi_{,x}=\rho_{\cdot}\ddot{}, \tag{20a}$$

$$A^g\psi_{,xx}+C^m\bar{\phi}_{,x}-C^m\psi=\rho_{11}\ddot{u}_{\quad}\ddot{} \quad . \tag{20b}$$

Note that in Eq. (20), ρ_{11} and ρ_{1111} are the inertia measures defined in Eq. (16).

For the equations of motion in Eq. (20), we assume plane wave solutions, solutions harmonic in both position, *x,* and time, *t*, expressed as

$$\bar{\phi}=\mathrm{Re}\left(Aie^{i(kx-\omega t)}\right), \quad \psi=\mathrm{Re}\left(Be^{i(kx-\omega t)}\right) \tag{21}$$

where k is the angular wavenumber, ω is the angular frequency, and $i^2 = -1$. Furthermore, A and B are the amplitudes and can assume complex values. Throughout this paper, "angular frequency" and "angular wavenumber" are referred to as "frequency" and "wavenumber" for brevity and have the units of radians per second and radians per meter, respectively. Upon substituting Eq. (21) in Eq. (20), the equations of motion can be recast in the following generalized eigenvalue problem

$$\begin{bmatrix} c_0^2 k^2 + c_A^2 k^2 & c_A^2 k \\ c_A^2 k & c_1^2 \varepsilon_1^2 k^2 + c_A^2 \end{bmatrix} \begin{bmatrix} A \\ B \end{bmatrix} = \omega^2 \begin{bmatrix} 1 & 0 \\ 0 & \varepsilon_1^2 + \varepsilon_2^4 k^2 \end{bmatrix} \begin{bmatrix} A \\ B \end{bmatrix}, \tag{22}$$

where we have defined the macro-scale, micro-scale relative deformation, and second gradient velocities c_0, c_A, and c_1, respectively, and two characteristic lengths ε_1 and ε_2, respectively, as

$$c_0^2 = \frac{C^M}{\rho}, \quad c_A^2 = \frac{C^m}{\rho}, \quad c_1^2 = \frac{A^g}{\rho_{11}}, \quad \varepsilon_1^2 = \frac{\rho_{11}}{\rho}, \quad \varepsilon_2^4 = \frac{\rho_{1111}}{\rho}. \tag{23}$$

Eq. (22) has nontrivial solution if

$$\left(c_0^2 k^2 + c_A^2 k^2 - \omega^2\right)\left(c_1^2 \varepsilon_1^2 k^2 + c_A^2 - \varepsilon_1^2 \omega^2 - \varepsilon_2^4 k^2 \omega^2\right) - c_A^4 k^2 = 0. \tag{24}$$

Equation (24) is the dispersion relation for the problem under study and can be considered as the solution for an eigenvalue problem with matrix form of equations given in Eq. (22) (see Refs. [50,51] for rigorous mathematical description regarding phononic eigenvalue problems). This equation relates the frequency and the wavenumber and can be utilized to obtain dispersion curves. However, it is useful to nondimensionalize Eq. (24). To this end, we define the characteristic time p, dimensionless velocities, γ_A, and γ_1, dimensionless term corresponding to inertial effect, χ, dimensionless frequency, η, and dimensionless wavenumber, ξ, as

$$p = \frac{\varepsilon_1}{c_0}, \quad \gamma_A = \frac{c_A}{c_0}, \quad \gamma_1 = \frac{c_1}{c_0}, \quad \chi = \frac{\varepsilon_2}{\varepsilon_1}, \quad \eta = p\omega, \quad \xi = \varepsilon_1 k. \tag{25}$$

Using Eq. (25), the dimensionless form of the dispersion relation in Eq. (24) is

$$\left(\eta^2 - \xi^2 - \gamma_A^2 \xi^2\right)\left(\eta^2 - \gamma_1^2 \xi^2 - \gamma_A^2 + \chi^4 \xi^2 \eta^2\right) - \gamma_A^4 \xi^2 = 0 \tag{26}$$

The maximum order of the dimensionless frequency η in Eq. (26) is four, meaning that there will be four solutions in the form $\eta = \eta(\xi)$. Two of the solutions are forward and the other two are backward wave branches. The forward and backward wave branches are symmetric with respect to the line $\eta = 0$ in the dispersion curve with horizontal and vertical axes as ξ and η, respectively. Therefore, we only consider the forward wave branches here. Furthermore, for each wave branch, the dimensionless phase velocity, v_p, and group velocity, v_g, are obtained as

$$v_p = \frac{\eta}{\xi}, \quad v_g = \frac{d\eta}{d\xi}. \tag{27}$$

Before analyzing the solutions of Eq. (26), it is fruitful to discuss the physical meaning of the parameters involved in Eq. (26). The dimensionless velocity γ_A is defined as the ratio of two velocities, whose definition can be simplified to $\gamma_A = \sqrt{\frac{C^m}{C^M}}$. As a result, γ_A, is a function of the macro-stiffness and micro-stiffness and represents the relative magnitude of micro-stiffness with respect to the macro-stiffness. The dimensionless velocity γ_1 can also be simplified to $\gamma_1 = \frac{1}{\varepsilon_1}\sqrt{\frac{A^g}{C^M}}$, where contrary to the dimensionless velocity γ_A, it is a function of both stiffnesses and inertia measures. The term $\sqrt{\frac{A^g}{C^M}}$ represents the static length scale for the current problem, therefore, the value of γ_1 is a ratio between the static and the dynamic length scale ε_1. Keeping the granular structure unchanged in terms of the distribution of masses, as the second gradient stiffness increases, so does the value for γ_1. On the other hand, keeping the stiffnesses of the granular material unchanged, as the second order inertia measure ρ_{11} increases (or equivalently as ε_1 increases), the value for γ_1 decreases. Finally, the expression for the dimensionless parameter χ can be recast as $\chi = \sqrt[4]{\frac{\rho\rho_{1111}}{\rho_{11}^2}}$, which encompasses the effect of inertia. For a case where the micro-scale mass density ρ' is constant, using Eq. (16), the expression for the dimensionless parameter χ is simplified to $\chi = 1.1583$. A different

distribution for the micro-scale mass density ρ' will result in different values for χ, as exemplified in Fig. 5 for a variety of micro-scale mass density distributions.

Returning to the dispersion relation in Eq. (26), we consider a granular medium with material constants $\gamma_A = 0.7$, $\gamma_1 = 10^{-6}$, and $\chi = 1.1583$ to explore the GMA predictions of wave propagation characteristics. The chosen values are taken to be representative of a case in which band gaps are present [9,15]. The solutions of Eq. (26) when solved for dimensionless frequency are plotted in the dispersion curve presented in Fig. 6a. There exists one acoustic branch starting at the origin, and one optical branch starting at a nonzero dimensionless frequency. The starting dimensionless frequency point for the optical branch can be obtained using Eq. (26) and substituting $\xi = 0$. This results in dimensionless frequency $\eta = \gamma_A$, as shown in Fig. 6a, or a real frequency $\omega = \sqrt{\frac{C^m}{\rho_{11}}}$. The asymptotes of the two wave branches can be obtained, discarding second order terms from Eq. (26), and solving for the dimensionless frequency. As a result, the asymptotes are

$$\eta = \sqrt{\gamma_A^2 + 1}\xi, \quad \eta = \frac{\gamma_1 \xi}{\sqrt{\chi^4 \xi^2 + 1}}, \tag{28}$$

or in terms of real frequency and wavenumber,

$$\omega = \sqrt{\frac{C^M + C^m}{\rho}}k, \quad \omega = \sqrt{\frac{A^g}{\rho_{1111}k^2 + \rho_{11}}}k \tag{29}$$

These asymptotes are shown in Fig. 6a. The asymptote $\eta = \sqrt{\gamma_A^2 + 1}\xi$ is a straight line and as seen in Fig. 6a, it fits the optical wave branch at large wavenumber and frequencies. On the other hand, the asymptote $\eta = \frac{\gamma_1 \xi}{\sqrt{\chi^4 \xi^2 + 1}}$ is not a straight line and shows the asymptotic value the acoustic wave branch takes. For the very small value of γ_1 taken in this example, this asymptote can be approximated by $\eta = 0$. This means that the acoustic branch ceases to propagate in very large wavenumbers (small wavelengths). For some frequency range depicted by a green box in

Fig. 6a, there is no real solution for the wavenumber. This frequency range is called frequency band gap (or stop band), and is associated with frequencies that do not propagate through the medium. Fig. 6b shows the phase and group velocities associated with the acoustic and optical branches. The difference between the phase and group velocities for each wave branch can cause a change in the shape of propagating pulse. The phase velocity values for both wave branches decrease as wavenumber becomes larger, therefore, the granular material with the assumed material parameters shows *normal dispersion*. One interesting observation in Fig. 6b is the existence of certain wavenumbers in which the signs of phase and group velocities corresponding to each wave branch are opposite. This phenomena is called negative group velocity (NGV) in the literature and is associated with backward propagation of the peak of the pulse [52]. From a physical viewpoint, NGV in a material with granular microstructure results from the resonance of sub-wavelength micro-structural elements (grain-scales) inherent in granular materials. From a mathematical viewpoint, the NGV results from the presence of the higher order inertia conjugate to rate of micro-deformation that appears in the presented continuum model, which leads to the term $\ddot{\psi}_{,xx}$ with both time and space derivatives in the equations of motion. As is seen in Fig. 6b, the NGV in the granular material is predicted to be wavenumber (frequency) dependent. Since group velocity is an integral entity depending on the collective behavior of a number of harmonics in relation to each other, the occurrence of NGV suggests smaller effective dispersion in the granular material [28]. To evaluate the physical mechanisms for the phenomena, we have performed parametric studies to investigate how the material parameters contribute to the appearance of NGV. Results (not shown here) revealed that for fixed values of γ_1 and χ, larger values of the parameter γ_A (or equivalently larger micro-scale stiffness C^m compared to a fixed value for the macro-scale stiffness C^M) result in increasing NGV. For fixed values of γ_A and χ, larger values of γ_1 (which represents the ratio of static and dynamic length scales) result in positive group velocity, while NGV is observed for small values of γ_1. For fixed values of γ_A and γ_1, larger values of χ predict higher NGV. To summarize, granular media with larger values of γ_A and χ, and smaller value for the parameter γ_1 are expected to show NGV in their optical branch. The parametric studies show that the NGV phenomena is controlled by the micro-deformation and its rate whose energy content can be modulated by parameters, γ_1, γ_A and χ. Importantly, these parameters represent the effect of

micro-mechano-morphology of granular material. For example, emergent micro-deformation phenomena for static case can be observed in defective granular structures as discussed in [47] or in granular structures with particular grain-pair interactions as in [16], as well as in discrete mass-spring models that include interactions with non-nearest neighbor [26,27]. It is also worthwhile to mention that NGV in longitudinal wave propagation has been observed in the context of axially moving materials with granular microstructure [10]. NGV phenomenon has also been predicted for transverse waves in granular systems with particular grain-pair interactions [9].

As mentioned earlier in the paper, the current format of equations of motion for the problem under study includes an additional term corresponding to the effect of higher order inertia. It is worthwhile to study how this additional term contributes to the wave propagation characteristics of granular medium. Therefore, we consider two cases, where in one case the higher order inertia ρ_{1111} is taken to be zero, reducing the equations of motion in Eq. (20) to the one adopted in [9], and in the other case the higher order inertia assumes a nonzero value and Eq. (20) holds fully. The dispersion curve of these cases are illustrated in Fig. 7a and are referred to as the current model and the reference model, respectively. In both cases we have used the same parameter constants used to produce the dispersion curve for Fig. 6, except for the dimensionless value χ, which in the reference model is zero and in the current model has been assumed 1.4 to enhance the contrast between the findings of the two models. Results in Fig. 7a reveal the fact that the additional term corresponding to higher order inertia affects the acoustic wave branch in large wavenumbers, while altering the behavior of the optical wave branch at small wavenumbers. In other words, the acoustic wave branches for the two models agree in small wavenumbers, and the optical wave branches for the two models agree in large wavenumbers. To investigate such observations, we consider two regions of wavenumbers. In small wavenumbers, Eq. (26) can be approximated by

$$\left(\chi^4\xi^2+1\right)\eta^4-\left(\left(\gamma_1^2+\gamma_A^2+1\right)\xi^2+\gamma_A^2\right)\eta^2+\gamma_A^2\xi^2=0\,. \tag{30}$$

Eq. (30) is a quadratic equation in η^2 and can be easily solved to give the equations for the acoustic and optical wave branches at small wavenumbers. For the optical branch, the first term on the left side in Eq. (30) is not small and contributes to the solution. This term contains the

information about the micro-scale mass density distribution, and therefore, the optical branch behavior is affected by the higher order inertia in small wavenumbers. For the acoustic branch, however, further simplifications can be made. Since the acoustic branch starts at zero frequency, the first term on the left side can be neglected. As a result, the frequency solution for the acoustic wave branch at small wavenumbers can be simplified to

$$\eta = \frac{\gamma_A \xi}{\sqrt{\left(\gamma_1^2 + \gamma_A^2 + 1\right)\xi^2 + \gamma_A^2}}. \tag{31}$$

As is clear from Eq. (31), the acoustic wave branch frequency solution is independent of higher order inertia effect in small wavenumbers. The same argument can be stated for the large wavenumber (small wavelength) behavior of the two wave branches using the asymptotes in Eq. (29). Clearly, the optical branch is independent of the higher order inertia in large wavenumbers, while the acoustic branch is affected by the higher order inertia.

We further note the change in stop band frequency range predicted by the two models, where the current model predicts stop band of frequencies lower than the one predicted by the reference model. Based on Fig. 7c and Fig. 7d, we note that, for the acoustic branch, the reference model predicts a diminishing positive group velocity and decreasing phase velocity for large wavenumbers, while the current model predicts a diminishing negative group velocity and vanishing phase velocity. For the optical wave branch, large wavenumber behavior of both models is the same, while in small wavenumbers, we observe that the current model predicts negative group velocity, which gradually reaches zero, and becomes positive as wavenumber increases. We further observe the change of location for the frequency stop bands in the two models, where the current model predicts lower frequency ranges for the band gaps, compared to the prediction of the reference model. While the model predictions can be extended to very large wavenumbers and frequencies, it is understood that the model predictions below wavelengths of the size of the RVE are not generally reliable as the homogenization is done in the scale of RVE. For example, for grains with diameters in the order of millimeters, and an RVE size in the order of 1000 grains, the dimensionless wavenumber limit of reliability on the theory predictions is less than 0.4. The reference model and current model predictions in the corresponding limiting wavenumber range are depicted in Fig. 7b. Finally, assuming negligible values for the

dimensionless parameters γ_1 and γ_A, the dispersion curve in Eq. (26) simplifies to the nondispersive relation $\eta = \xi$ which in terms of real frequency and wavenumber reads $\omega = c_0 k$. Therefore, the model developed here simplifies to a classical model.

4. Conclusions

In this paper, we have theoretically investigated the elastic wave dispersion characteristics in an infinite 1D continua with granular microstructure. We have focused on the effect of higher order inertia terms that appear in the enhanced micromorphic model based upon GMA [6]. The additional term, which is absent in the previous formats of micromorphic models of degree 1 (including those presented by the authors [8–10,15]), has a profound effect on the dynamic behavior of granular media. The results presented in the current paper, when compared to the previous model results, show, not only better agreement with the wave propagation characteristics observed experimentally and numerically in the literature, e.g., in [17,53,54], but predict additional effects. In particular, the higher order inertia terms most-noticeably affect the prediction of the optical wave branch behavior. It is remarkable that the higher-order inertia terms are controlled by the micro-scale mass density distribution in the RVE. Thus, it is possible to conceive of homogeneous materials with the same macro-scale mass density and different higher-order inertia. In these materials, the re-allocation of kinetic energies in the micro- and macro-scale degrees of freedom can introduce interesting modulation of wave propagation. The theoretical results reported in this paper can be a precursor and motivation for an experimental effort, which can otherwise be difficult to conceive, plan and execute given the multitude factors that can affect wave propagation and their measurements. Moreover, these theoretical results can promote the development of dynamic identification procedure that can be applied for simulating wave propagation in random granular assemblies across a wide range of frequencies. We note that the existing dynamic discrete models typically include dissipation, such that the intermixing of microstructural, micro-inertial and imposed dissipation effects confounds the results of wave propagation simulations.

The micromorphic based continuum model presented in this paper assumes non-dissipative linear behavior in micro- and macro-scales. While many granular systems feature nonlinear

grain-pair interactions, understanding linear elastic behavior has practical significance for small amplitude vibrations, where assuming a quadratic potential is valid. Furthermore, the considered model is specialized for infinitesimal deformations, and therefore, it is applicable to small amplitude vibrations.

For an accurate description of a material with granular microstructure, one needs complete information about the micro-mechano-morphological aspect of the granular material, e.g., the position, size, and shape of the grains, their inertial properties, and the interaction mechanisms between all grains in contact. GMA treats the problem in an averaged sense by reducing the number of parameters from thousands (if not millions) to a few continuum material constants. The analysis presented in the current paper can be potentially used to identify the continuum material parameters of granular media from experiments or numerical simulations. To describe a one-dimensional material with granular microstructure using GMA introduced in the paper and the assumed form of deformation energy densities, one needs to identify 6 material constants. These constant are the macro-scale mass density, ρ, micro-scale mass density, ρ', and the knowledge on its distribution (which results in the dependent inertia measures ρ_{11} and ρ_{1111}), the RVE size, L, the macro-scale stiffness, C^M, the micro-scale stiffness, C^m, and the second gradient stiffness, A^g. These 6 material parameters can be identified by performing a constrained optimization problem with the cost function being the difference between the results of the predictions of the theory and the experimental or discrete simulation results. A similar approach can be found in [29,55,56] where the material constants of a micromorphic model were determined based on experimental, atomistic, or finite element simulation results through phonon dispersion relations. We also note the identification methods discussed for static elastic properties in [47,57].

Furthermore, it is noteworthy that while atomistic and discrete simulations can describe the dispersive behavior of materials in very short wavelengths (large wavenumbers), when compared to such simulations, a micromorphic-based continuum model is able to describe the behavior of materials with good accuracy up to wavelengths suitably larger than the corresponding characteristic length of the system [29,56]. For smaller wavelengths, the accuracy of the results decreases and the predictions of the theory needs further investigation by comparison with experimental or discrete simulation results. It is encouraging to note that, the predicted zero

group velocity in the optical branch suggesting non-propagating wave mode, has been observed for granular crystals with nonlinear grain-pair interactions in hybridized modes [58]. The use of the GMA based micromorphic model expands the applicability of continuum models to regions beyond what classical continuum mechanics is able to predict, while revealing the relevant micro-mechanisms.

It is evident that the current approach is useful for not only describing the dynamic behavior of natural granular materials, but the methodology can be applied to design granular metamaterials for vibration mitigation purposes. Notably, such design can utilize granular-structure, grain-pair interaction properties as well as the micro-scale mass density effects in the macro-scale behavior of such media. We further note that since the GMA links the grain-scale behavior to the macro-scale consisting of millions of particles, the resultant continuum model provides a systematic approach to explore the influences of both micro- and macro-scale parameters, which often have confounding and contradicting effects on the wave propagation behavior. We also note that a large number of published literature is focused upon problems that are restricted to study the systems with unit cells of one or very few grains, with limited variation in grain composition [17,53,54,59–61] The advancements in additive manufacturing technology, however, allows us to envision and realize granular metamaterials with specified micro-scale mass density distributions resulting in tailored vibration characteristics predicted in the present paper. Further verification of the continuum predictions presented here will be performed using discrete simulations with grains in future publications.

Statement of Competing Interest

Authors have no competing interests to declare.

Acknowledgements

This research is supported in part by the United States National Science Foundation grant CMMI -1727433.

References

[1] Kim E, Yang J. Review: Wave propagation in granular metamaterials. Funct Compos Struct 2019;1:012002. doi:10.1088/2631-6331/ab0c7e.

[2] Gantzounis G, Serra-Garcia M, Homma K, Mendoza JM, Daraio C. Granular metamaterials for vibration mitigation. J Appl Phys 2013;114. doi:10.1063/1.4820521.

[3] Turco E, Dell'Isola F, Misra A. A nonlinear Lagrangian particle model for grains assemblies including grain relative rotations. Int J Numer Anal Methods Geomech 2019;43:1051–79. doi:10.1002/nag.2915.

[4] Cundall PA, Strack ODL. A discrete numerical model for granular assemblies. Geotechnique 1979;29:47–65.

[5] Cheng H, Luding S, Saitoh K, Magnanimo V. Elastic wave propagation in dry granular media: Effects of probing characteristics and stress history. Int J Solids Struct 2020;187:85–99. doi:10.1016/j.ijsolstr.2019.03.030.

[6] Nejadsadeghi N, Misra A. Extended granular micromechanics approach: a micromorphic theory of degree n. Math Mech Solids 2019:108128651987947. doi:10.1177/1081286519879479.

[7] Poorsolhjouy P, Misra A. Granular micromechanics based continuum model for grain rotations and grain rotation waves. J Mech Phys Solids 2019;129:244–60. doi:10.1016/J.JMPS.2019.05.012.

[8] Nejadsadeghi N, Placidi L, Romeo M, Misra A. Frequency band gaps in dielectric granular metamaterials modulated by electric field. Mech Res Commun 2019;95. doi:10.1016/j.mechrescom.2019.01.006.

[9] Misra A, Nejadsadeghi N. Longitudinal and transverse elastic waves in 1D granular materials modeled as micromorphic continua. Wave Motion 2019;90:175–95. doi:10.1016/j.wavemoti.2019.05.005.

[10] Nejadsadeghi N, Misra A. Axially moving materials with granular microstructure. Int J Mech Sci 2019;161–162:105042. doi:10.1016/j.ijmecsci.2019.105042.

[11] Sadd MH, Tai Q, Shukla A. Contact law effects on wave propagation in particulate materials using distinct element modeling. Int J Non Linear Mech 1993;28:251–65. doi:10.1016/0020-7462(93)90061-O.

[12] Papargyri-Beskou S, Mylonakis G. Wave dispersion studies in granular media by analytical and analytical-numerical methods. Soil Dyn Earthq Eng 2009;29:883–7. doi:10.1016/j.soildyn.2008.10.003.

[13] Berezovski A, Engelbrecht J, Salupere A, Tamm K, Peets T, Berezovski M. Dispersive waves in microstructured solids. Int J Solids Struct 2013;50:1981–90. doi:10.1016/j.ijsolstr.2013.02.018.

[14] Pal RK, Waymel RF, Geubelle PH, Lambros J. Tunable Wave Propagation in Granular Crystals by Altering Lattice Network Topology. J Eng Mater Technol Trans ASME 2017;139. doi:10.1115/1.4034820.

[15] Misra A, Poorsolhjouy P. Granular micromechanics based micromorphic model predicts frequency band gaps. Contin Mech Thermodyn 2016;28:215–34. doi:10.1007/s00161-015-0420-y.

[16] Misra A, Nejadsadeghi N, De Angelo M, Placidi L. Chiral metamaterial predicted by granular micromechanics: verified with 1D example synthesized using additive manufacturing. Contin Mech Thermodyn 2020. doi:10.1007/s00161-020-00862-8.

[17] Wei LS, Wang YZ, Wang YS. Nonreciprocal transmission of nonlinear elastic wave metamaterials by incremental harmonic balance method. Int J Mech Sci 2020;173:105433. doi:10.1016/j.ijmecsci.2020.105433.

[18] Kosevich AM. On a simple model of the photonic or phononic crystal. JETP Lett 2001;74:559–63. doi:10.1134/1.1450291.

[19] Acoust SR-SP, 1956 undefined. Acoustical properties of a thinly laminated medium n.d.

[20] Hussein MI, Leamy MJ, Ruzzene M. Dynamics of phononic materials and structures: Historical origins, recent progress, and future outlook. Appl Mech Rev 2014;66. doi:10.1115/1.4026911.

[21] Fredkin DR, Ron A. Effectively left-handed (negative index) composite material. Appl Phys Lett 2002;81:1753–5. doi:10.1063/1.1505119.

[22] Lee SH, Park CM, Seo YM, Wang ZG, Kim CK. Composite acoustic medium with simultaneously negative density and modulus. Phys Rev Lett 2010;104:054301. doi:10.1103/PhysRevLett.104.054301.

[23] Slesarenko V, Galich PI, Li J, Fang NX, Rudykh S. Foreshadowing elastic instabilities by negative group velocity in soft composites. Appl Phys Lett 2018;113:031901. doi:10.1063/1.5042077.

[24] Nemat-Nasser S, Willis JR, Srivastava A, Amirkhizi A V. Homogenization of periodic elastic composites and locally resonant sonic materials. Phys Rev B - Condens Matter Mater Phys 2011;83:104103. doi:10.1103/PhysRevB.83.104103.

[25] Minagawa S, Nemat-Nasser S. Harmonic waves in three-dimensional elastic composites. Int J Solids Struct 1976;12:769–77. doi:10.1016/0020-7683(76)90041-X.

[26] Wang J, Huang Y, Chen W, Zhu W. Abnormal wave propagation behaviors in two-dimensional mass–spring structures with nonlocal effect. Math Mech Solids 2019;24:3632–43. doi:10.1177/1081286519853606.

[27] Wang J, Zhou W, Huang Y, Lyu C, Chen W, Zhu W. Controllable wave propagation in a weakly nonlinear monoatomic lattice chain with nonlocal interaction and active control. Appl Math Mech (English Ed 2018;39:1059–70. doi:10.1007/s10483-018-2360-6.

[28] Tamm K, Peets T, Engelbrecht J, Kartofelev D. Negative group velocity in solids. Wave Motion 2017;71:127–38. doi:10.1016/J.WAVEMOTI.2016.04.010.

[29] Chen Y, Lee JD. Determining material constants in micromorphic theory through phonon dispersion relations. Int J Eng Sci 2003;41:871–86. doi:10.1016/S0020-7225(02)00321-X.

[30] Mindlin RD. Micro-structure in linear elasticity. Arch Ration Mech Anal 1964;16:51–78. doi:10.1007/BF00248490.

[31] Madeo A, Neff P, Ghiba I-D, Placidi L, Rosi G. Band gaps in the relaxed linear micromorphic continuum. ZAMM - J Appl Math Mech / Zeitschrift Für Angew Math Und Mech 2015;95:880–7. doi:10.1002/zamm.201400036.

[32] Madeo A, Neff P, Ghiba ID, Placidi L, Rosi G. Wave propagation in relaxed micromorphic continua: modeling metamaterials with frequency band-gaps. Contin Mech Thermodyn 2015;27:551–70. doi:10.1007/s00161-013-0329-2.

[33] Rosi G, Placidi L, Auffray N. On the validity range of strain-gradient elasticity: A mixed static-dynamic identification procedure. Eur J Mech A/Solids 2018;69:179–91. doi:10.1016/j.euromechsol.2017.12.005.

[34] Eremeyev VA, Rosi G, Naili S. Comparison of anti-plane surface waves in strain-gradient materials and materials with surface stresses. Math Mech Solids 2019;24:2526–35. doi:10.1177/1081286518769960.

[35] Rosi G, Auffray N. Anisotropic and dispersive wave propagation within strain-gradient framework. Wave Motion 2016;63:120–34. doi:10.1016/j.wavemoti.2016.01.009.

[36] Ben-Amoz M. A dynamic theory for composite materials. Zeitschrift Für Angew Math Und Phys ZAMP 1976;27:83–99. doi:10.1007/BF01595244.

[37] Doney RL, Agui JH, Sen S. Energy partitioning and impulse dispersion in the decorated, tapered, strongly nonlinear granular alignment: A system with many potential applications. J Appl Phys 2009;106. doi:10.1063/1.3190485.

[38] Doney RL, Sen S. Impulse absorption by tapered horizontal alignments of elastic spheres. Phys Rev E - Stat Nonlinear, Soft Matter Phys 2005;72. doi:10.1103/PhysRevE.72.041304.

[39] Wang J, Chu X, Zhang J, Liu H. The effects of microstructure on wave velocity and wavefront in granular assemblies with binary-sized particles. Int J Solids Struct 2019;159:156–62. doi:10.1016/j.ijsolstr.2018.09.026.

[40] Germain P. The Method of Virtual Power in Continuum Mechanics. Part 2: Microstructure. SIAM J Appl Math 1973;25:556–75. doi:10.1137/0125053.

[41] dell'Isola F, Seppecher P, Alibert JJ, Lekszycki T, Grygoruk R, Pawlikowski M, et al. Pantographic metamaterials: an example of mathematically driven design and of its technological challenges. Contin Mech Thermodyn 2019;31:851–84. doi:10.1007/s00161-018-0689-8.

[42] Giorgio I, Grygoruk R, Dell'Isola F, Steigmann DJ. Pattern formation in the three-dimensional deformations of fibered sheets. Mech Res Commun 2015;69:164–71. doi:10.1016/j.mechrescom.2015.08.005.

[43] Giorgio I, Rizzi NL, Turco E. Continuum modelling of pantographic sheets for out-of-plane bifurcation and vibrational analysis. Proc R Soc A Math Phys Eng Sci 2017;473. doi:10.1098/rspa.2017.0636.

[44] Abdoul-Anziz H, Seppecher P. Strain gradient and generalized continua obtained by homogenizing frame lattices. Math Mech Complex Syst 2018;6:213–50. doi:10.2140/memocs.2018.6.213.

[45] Alibert J-J, Seppecher P, Dell'Isola F. Truss Modular Beams with Deformation Energy Depending on Higher Displacement Gradients. Math Mech Solids 2003;8:51–73. doi:10.1177/1081286503008001658.

[46] Seppecher P, Alibert JJ, Isola FD. Linear elastic trusses leading to continua with exotic mechanical interactions. J. Phys. Conf. Ser., vol. 319, Institute of Physics Publishing; 2011. doi:10.1088/1742-6596/319/1/012018.

[47] Misra A, Poorsolhjouy P. Identification of higher-order elastic constants for grain assemblies based upon granular micromechanics. Math Mech Complex Syst 2015;3:285–308. doi:10.2140/memocs.2015.3.285.

[48] Essén H. Average angular velocity. Eur J Phys 1993;14:201–5. doi:10.1088/0143-0807/14/5/002.

[49] Bacigalupo A, Gambarotta L. Second-gradient homogenized model for wave propagation in heterogeneous periodic media. Int J Solids Struct 2014;51:1052–65. doi:10.1016/j.ijsolstr.2013.12.001.

[50] Mokhtari AA, Lu Y, Srivastava A. On the properties of phononic eigenvalue problems. J Mech Phys Solids 2019;131:167–79. doi:10.1016/j.jmps.2019.07.005.

[51] Mokhtari AA, Lu Y, Srivastava A. On the emergence of negative effective density and modulus in 2-phase phononic crystals. J Mech Phys Solids 2019;126:256–71. doi:10.1016/j.jmps.2019.02.016.

[52] Gehring GM, Schweinsberg A, Barsi C, Kostinski N, Boyd RW. Observation of Backward Pulse Propagation Through a Medium with a Negative Group Velocity. Science (80-) 2006;312:895 LP – 897. doi:10.1126/science.1124524.

[53] Boechler N, Yang J, Theocharis G, Kevrekidis PG, Daraio C. Tunable vibrational band gaps in one-dimensional diatomic granular crystals with three-particle unit cells. J. Appl. Phys., vol. 109, 2011. doi:10.1063/1.3556455.

[54] Jensen JS. Phononic band gaps and vibrations in one- and two-dimensional mass-spring structures. J Sound Vib 2003;266:1053–78. doi:10.1016/S0022-460X(02)01629-2.

[55] Madeo A, Collet M, Miniaci M, Billon K, Ouisse M, Neff P. Modeling phononic crystals via the weighted relaxed micromorphic model with free and gradient micro-inertia. J Elast 2018;130:59–83. doi:10.1007/s10659-017-9633-6.

[56] Zeng X, Chen Y, Lee JD. Determining material constants in nonlocal micromorphic theory through phonon dispersion relations. Int J Eng Sci 2006;44:1334–45. doi:10.1016/j.ijengsci.2006.08.002.

[57] Placidi L, Andreaus U, Corte A Della, Lekszycki T. Gedanken experiments for the determination of two-dimensional linear second gradient elasticity coefficients. Zeitschrift Fur Angew Math Und Phys 2015;66:3699–725. doi:10.1007/s00033-015-0588-9.

[58] Zhang Q, Venegas R, Umnova O, Lan Y. Tuning coupled wave dispersion in a granular chain on a V-shaped rail. Wave Motion 2019;90:51–65. doi:10.1016/j.wavemoti.2019.04.009.

[59] Chong C, Porter MA, Kevrekidis PG, Daraio C. Nonlinear coherent structures in granular crystals. J Phys Condens Matter 2017;29. doi:10.1088/1361-648X/aa7672.

[60] Ghavanloo E, Fazelzadeh SA, Rafii-Tabar H. Formulation of an efficient continuum mechanics-based model to study wave propagation in one-dimensional diatomic lattices. Mech Res Commun 2020;103. doi:10.1016/j.mechrescom.2019.103467.

[61] Fraternali F, Porter MA, Daraio C. Optimal design of composite granular protectors. Mech Adv Mater Struct 2010;17:1–19. doi:10.1080/15376490802710779.

List of Figures

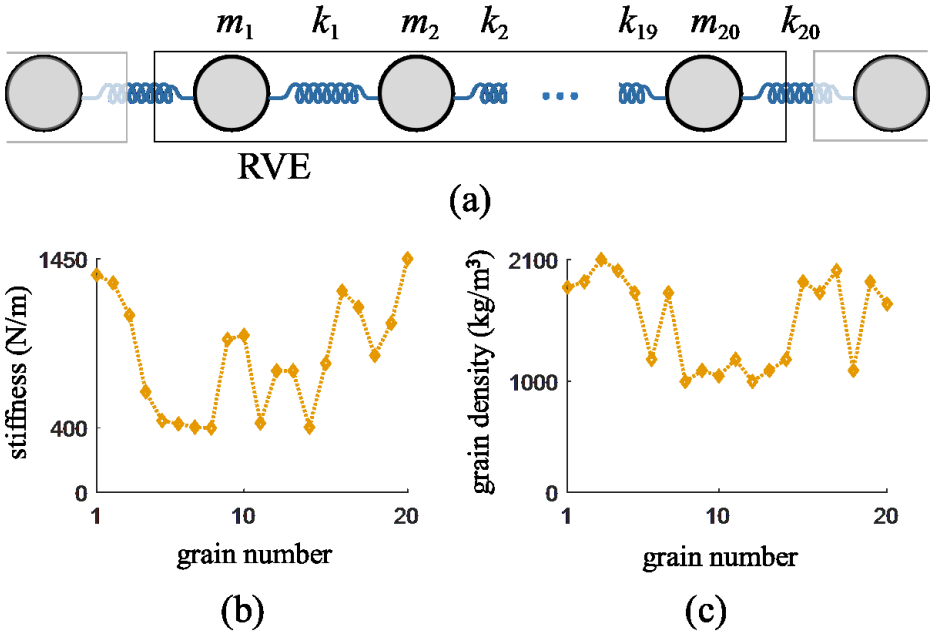

Fig 1. (a) Schematic of the 1D RVE modeled as masses and springs, (b) the variation in the grain-pair stiffness in the RVE, and (c) the variation in the grain mass density in the RVE.

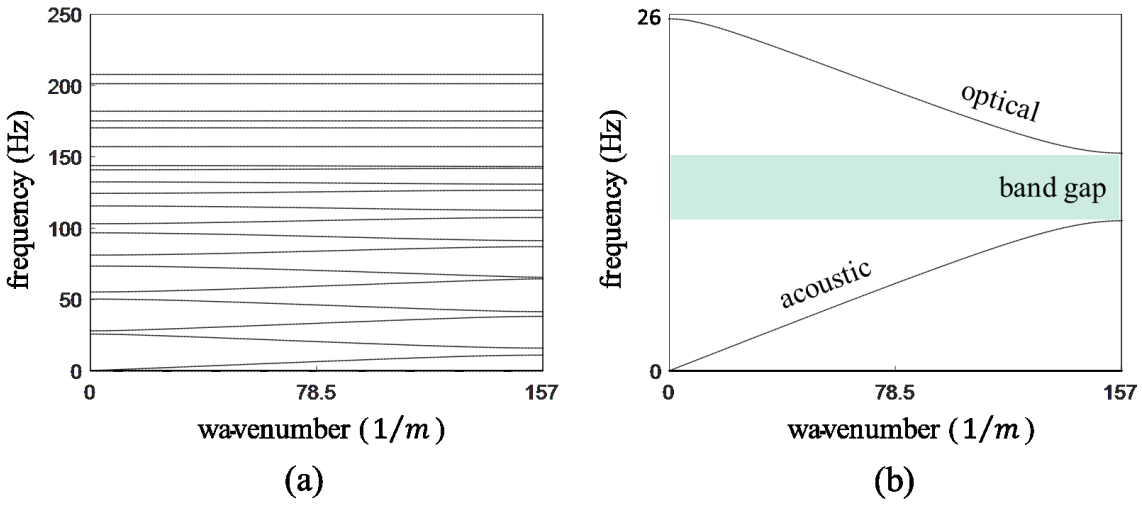

Fig 2. (a) Dispersion curve from discrete simulation of the granular structure modeled as masses and springs, and (b) the first two wave branches in the dispersion curve from discrete simulation of the granular structure.

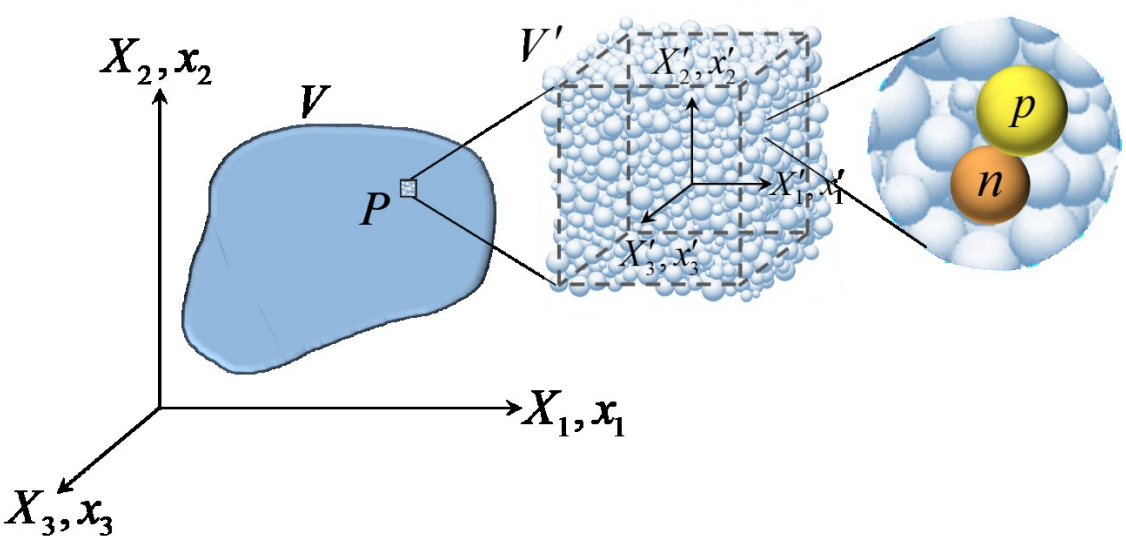

Fig 3. Schematic of the continuum material point, *P*, and its granular microstructure magnified for better visualization, where the *x'* coordinate system is attached to its center of mass.

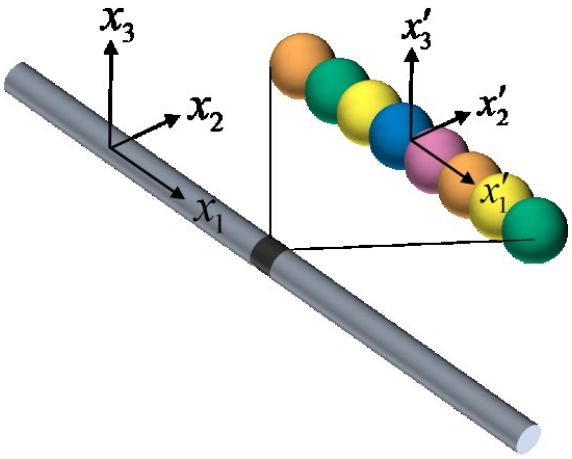

Fig 4. Schematic of a 1D continuum in x_1 direction with granular micro-structure in x'_1 direction. A material point in the macro-scale coordinate system is a collection of grains that can differ in micro-density, micro-morphology and micro-mechanical properties, represented here by grains with different colors.

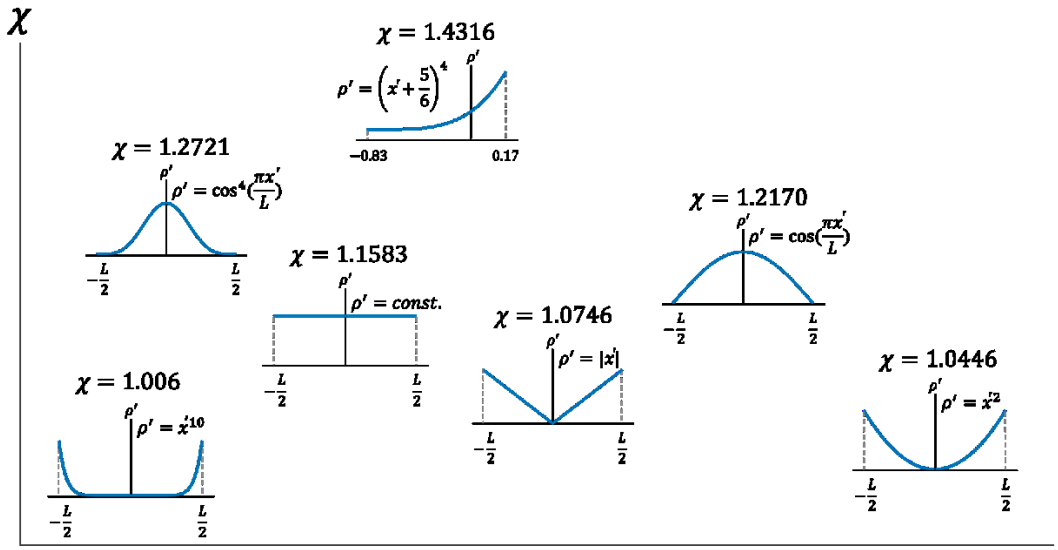

Fig 5. Examples of possible micro-scale mass density ρ' distributions in a 1D RVE and their correspondent dimensionless value χ.

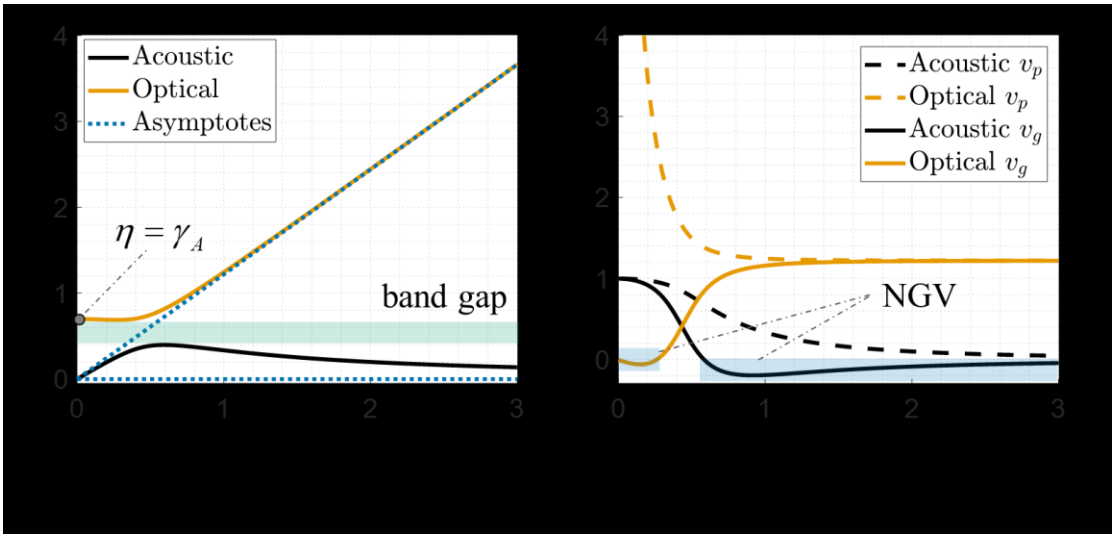

Fig 6. (a) Dispersion curve for a 1D material with granular microstructure. (b) Phase and group velocities for acoustic and optical wave branches in a 1D material with granular microstructure.

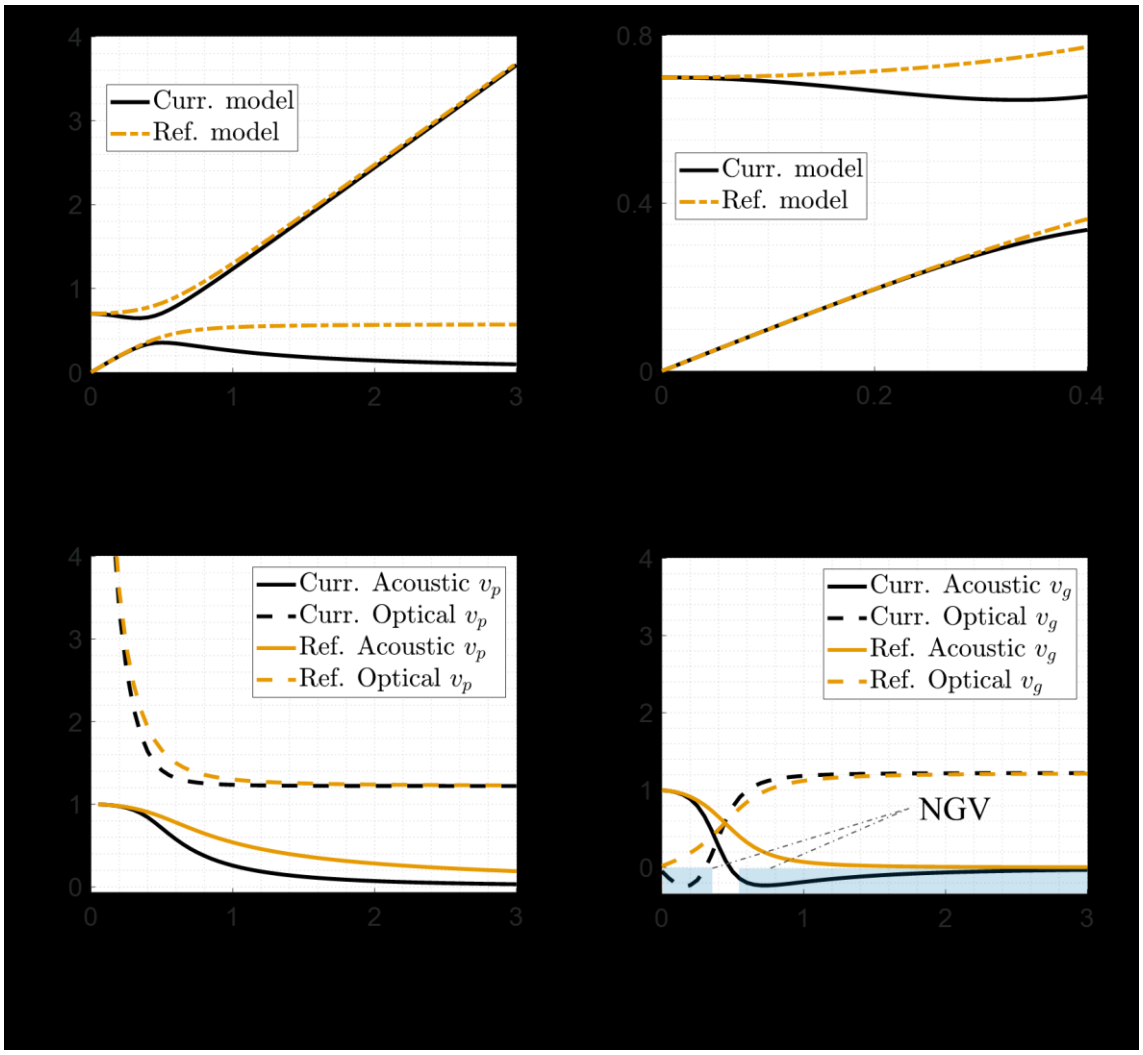

Fig 7. Dispersion curve comparison between the reference (Ref.) model in [9] and the current (Curr.) model in (a) dimensionless wavenumbers ranging from 0 to 3, and (b) dimensionless wavenumbers ranging from 0 to 0.4. (c) Phase velocity comparison between the reference model and the current model. (d) Group velocity comparison between the reference model and the current model.